

## DISTRIBUTIONS IN THE PROCESS $e^+e^- \rightarrow \mu^+\mu^-(\gamma)$

F.A. BERENDS and R. KLEISS

*Deutsches Elektronen-Synchrotron DESY, Hamburg, Germany  
and  
Instituut-Lorentz, Leiden, The Netherlands*

Received 25 July 1980

Analytical expressions for a number of distributions in the process  $e^+e^- \rightarrow \mu^+\mu^-(\gamma)$  are given. A procedure is outlined to simulate events for this reaction by using the analytical distributions. This method then numerically provides any other distribution and makes it possible to impose any experimental constraint to radiative correction calculations. Besides examples for pure QED situations, the corrections to  $R$  and to the thrust distribution for hadronic events are also discussed.

### 1. Introduction

The processes

$$e^+(p_+) + e^-(p_-) \rightarrow \mu^+(q_+) + \mu^-(q_-), \quad (1.1)$$

$$e^+(p_+) + e^-(p_-) \rightarrow \mu^+(q_+) + \mu^-(q_-) + \gamma(k), \quad (1.2)$$

are of interest for various reasons. In the first place they test the standard model [1] of unified electroweak interactions. Secondly, the theoretical treatment of (1.1) and (1.2) can be carried over to a final state with two jets with bremsstrahlung of a photon or gluon.

For testing electroweak interactions one concentrates on the forward-backward asymmetry of reaction (1.1). It is, however, unavoidable that events of reaction (1.2) contribute to this quantity. For the case where the muon events are selected on the basis of a threshold energy ( $E_{th}$ ) and acollinearity angle ( $\zeta$ ) requirement, this has been dealt with in the literature [2, 3]. The differential cross section  $d\sigma/d\Omega_\mu$  for reaction (1.1) is obtained up to order  $\alpha^3$  and depends on the parameters  $E_{th}$  and  $\zeta$ , which determine the allowed phase space for reaction (1.2). Over the latter phase space a three-dimensional integration is carried out numerically. The weak mixing angle can then be extracted from the experimental data.

Although the energy and acollinearity requirements are quite reasonable, it would be better for the analysis of experiments to have radiative correction calculations which are applicable in more general situations. The most natural solution is to have a numerical method to simulate events of reaction (1.1) and (1.2) at the same time. The  $N$  generated events must be such that they approximate the multidifferential cross sections for (1.1) and (1.2), when  $N$  becomes large. The events which have

momenta such that they could not be seen in a specific experiment can then be omitted. Of the remaining events, one knows the cross section and therefore the radiative correction. Of course, the event generator can also be used to evaluate the cross section for those events which would never simulate a cross section for reaction (1.1), e.g., very acollinear or acoplanar events.

When reactions (1.1) and (1.2) are considered with quarks in the final state, certain QCD relevant quantities like  $R$  or a thrust distribution for jets are extracted from the data. Since a good knowledge of these quantities for tests of QCD is important, the initial state radiation of a photon should accurately be taken into account. This is particularly so, since often the initial state QED correction is of the same order of magnitude as the physically more interesting final state QCD correction.

It turns out that the analytical knowledge of a certain number of distributions makes a numerical generation of events possible. In principle, various choices for these distributions can be made. If one is only interested in either initial state radiation or final state radiation, choices for the distributions can be made for which it is easy to find analytical expressions. In the case, where one is also interested in the interference between initial state and final state radiation, a compromise in the choice of variables has to be made. We shall calculate analytically  $d\sigma/d\Omega_\mu dk$ , where  $\Omega_\mu$  is the solid angle of the  $\mu^+$  and  $k$  is the photon energy. This distribution has the advantage that it can be directly used for a one-dimensional numerical integration over  $k$  to give the radiative corrections to  $d\sigma/d\Omega_\mu$ , depending on  $E_{\text{th}}$  and  $\zeta$ . This is faster than the previous more-dimensional integration method for the same quantity [2, 3].

The outline of the paper is as follows. In sect. 2 the known virtual corrections and bremsstrahlung cross section are summarized. In sect. 3 a number of analytic formulae for distributions and for the total cross section are given. Sect. 4 describes the scheme used for the generation of events. In sect. 5 a number of numerical results are presented, e.g., acollinearity and acoplanarity distributions and radiative corrections to  $d\sigma/d\Omega_\mu$ .

## 2. Virtual corrections and bremsstrahlung

Expressions for the virtual and soft bremsstrahlung correction to reaction (1.1) can be found in ref. [4]. The sum of both corrections is expressed in a correction  $\delta_A$ , where A denotes the fact that the correction is known analytically:

$$\frac{d\sigma}{d\Omega_\mu} = \frac{d\sigma_0}{d\Omega_\mu} (1 + \delta_A), \quad (2.1)$$

where the lowest order cross section is given by

$$\frac{d\sigma_0}{d\Omega_\mu} = \frac{\alpha^2}{4s} (1 + c^2), \quad (2.2)$$

with  $c = \cos \theta$ ,  $\theta$  being the angle between  $e^+$  and  $\mu^+$ .

The correction  $\delta_A$  can be written as

$$\begin{aligned} \delta_A &= (\beta_i + \beta_f + \beta_{\text{int}}) \ln\left(\frac{k_1}{E}\right) + \frac{2\alpha}{\pi} \left\{ \frac{13}{12} \left( \ln \frac{s}{m_e^2} + \ln \frac{s}{m_\mu^2} \right) + \frac{1}{3}\pi^2 - \frac{28}{9} \right. \\ &\quad - \frac{2}{1+c^2} [c(\ln^2(\sin \frac{1}{2}\theta) + \ln^2(\cos \frac{1}{2}\theta)) + \sin^2 \frac{1}{2}\theta \ln(\cos \frac{1}{2}\theta) - \cos^2 \frac{1}{2}\theta \ln(\sin \frac{1}{2}\theta)] \\ &\quad \left. + 2 \ln^2(\sin \frac{1}{2}\theta) - 2 \ln^2(\cos \frac{1}{2}\theta) - \text{Li}_2(\sin^2 \frac{1}{2}\theta) + \text{Li}_2(\cos^2 \frac{1}{2}\theta) \right\} \\ &= \beta \ln\left(\frac{k_1}{E}\right) + \delta_{\text{AR}}, \end{aligned} \tag{2.3}$$

with

$$\begin{aligned} \beta &= \beta_i + \beta_f + \beta_{\text{int}}, \\ \beta_i &= \frac{2\alpha}{\pi} \left( \ln \frac{s}{m_e^2} - 1 \right), \\ \beta_f &= \frac{2\alpha}{\pi} \left( \ln \frac{s}{m_\mu^2} - 1 \right), \\ \beta_{\text{int}} &= \frac{8\alpha}{\pi} \ln(\tan \frac{1}{2}\theta), \end{aligned} \tag{2.4}$$

$m_e$  and  $m_\mu$  being the electron and muon mass, and  $\text{Li}_2$  denoting the dilogarithm. The expression for  $\delta_A$  contains contributions from the vertex corrections, the vacuum polarization due to an electron and muon loop, and two box diagrams. Moreover, the soft isotropically emitted bremsstrahlung up to a maximum photon energy  $k_1$  is contained in  $\delta_A$ . In the evaluation of  $\delta_A$  it is assumed that

$$\sin \theta \gg m_\mu/E, \quad m_\mu/E \ll 1. \tag{2.5}$$

More involved expressions not using this approximation can be found in ref. [3].

The values  $k_1$  for which  $\delta_A$  is a good approximation to the radiative corrections are limited from below by the necessity of exponentiation and from above by the necessity of taking hard bremsstrahlung into account.

For too small values of  $k_1$ ,  $\delta_A$  becomes large and negative such that it becomes necessary to estimate higher order corrections, which is done by exponentiation of the leading log part of  $\delta_A$ . One then takes as an approximative formula to the corrections

$$\frac{d\sigma}{d\Omega_\mu} = \frac{d\sigma_0}{d\Omega_\mu} (1 + \delta_{\text{AR}}) \left( \frac{k_1}{E} \right)^\beta. \tag{2.6}$$

For too large values of  $k_1$  the factorized matrix element for the bremsstrahlung which

is used in the derivation of (2.3) is no longer a good approximation for the real (hard) bremsstrahlung. An idea of the  $k$  values for which this happens can be derived from an expression for the total cross section for reactions (1.1) and (1.2), given in sect. 3. One finds for the difference between the exact total cross section and the one evaluated on the basis of the soft photon approximation

$$\sigma_{\text{exact}} - \sigma_{\text{soft}} = \frac{2\alpha}{\pi} \sigma_0 \left( -\frac{k}{E} \ln \frac{s}{m_\mu^2} + \mathcal{O}\left(\frac{k^2}{E^2}\right) \right), \quad (2.7)$$

where the lowest order total cross section

$$\sigma_0 = \frac{4\alpha^2 \pi}{3s} \quad (2.8)$$

is factorized out. The requirement that this difference is less than 1% of  $\sigma_0$  gives, for energies where  $m_\mu/E \ll 1$ ,

$$\frac{k}{E} < 0.01 \times \frac{\pi}{2\alpha} \left( \ln \frac{s}{m_\mu^2} \right)^{-1}, \quad (2.9)$$

e.g.,  $k/E \leq 0.18$  for  $E = 20$  GeV.

To eq. (2.6) other contributions should be added, namely the vacuum polarization due to a  $\tau$ -loop ( $\delta_\tau$ ), the one due to hadrons ( $\delta_{\text{had}}$ ), and Z- $\gamma$  interference from the electroweak interactions. These contributions are

$$\delta_\tau = \frac{2\alpha}{\pi} \left( \frac{1}{3} \ln \frac{s}{m_\tau^2} - \frac{5}{9} \right), \quad (2.10)$$

where  $m_\tau = 1782$  MeV,

$$\delta_{\text{had}} = -2 \operatorname{Re} \prod_{\text{h}}(s) = \frac{s}{2\pi^2 \alpha} \int_{4m_\pi^2}^{\infty} \frac{\sigma(s')}{s-s'} ds', \quad (2.11)$$

where the dispersion integral over the total  $e^+e^-$  hadronic cross section has to be evaluated numerically [5].

The weak-electromagnetic interference cross section takes the form

$$\frac{d\sigma^{\text{W}}}{d\Omega_\mu} = \frac{\alpha^2}{4s} 2\chi (g_V^2(1+c^2) + 2g_A^2 c), \quad (2.12)$$

where

$$\begin{aligned} \chi &= g \frac{sM_Z^2}{s-M_Z^2}, \\ M_Z^2 &= (4g \sin^2(2\theta_w))^{-1}, \\ g_V &= -1 + 4 \sin^2 \theta_w, \\ g_A &= -1, \\ g &= 4.4 \times 10^{-11} \text{ MeV}^{-2}. \end{aligned} \quad (2.13)$$

This weak effect can be expressed in terms of

$$\delta_W = \left( \frac{d\sigma^W}{d\Omega_\mu} \right) / \left( \frac{d\sigma_0}{d\Omega_\mu} \right), \tag{2.14}$$

which has to be added to  $\delta_{AR}$  in eqs. (2.3) or (2.6).

This is the only place where the weak interactions occur in the present treatment. For PETRA/PEP energies this is sufficient. For higher energies it first becomes necessary to deal with the full Z-exchange amplitude and the QED corrections (virtual and bremsstrahlung) to it, then also to take the width of the Z in the propagator into account, and finally to apply the weak virtual corrections to the QED amplitude [6].

Besides the expressions for virtual and soft bremsstrahlung corrections we need the hard bremsstrahlung cross sections. Two choices of the kinematical variables will be convenient, one set consisting of solid angles of  $\mu^+$  and  $\gamma$  and the photon energy  $k$ , another set using the solid angle of the  $\mu^+$ , an azimuthal angle of the photon and the energies  $q_+, q_-$  of the  $\mu^+$  and  $\mu^-$ , respectively. We have

$$\frac{d\sigma^B}{d\Omega_\mu d\Omega_\gamma dk} = \frac{\alpha^3}{2\pi^2 s} \frac{|q_+|k}{2p_+^0 - k + k \cos \theta_\gamma} A, \tag{2.15}$$

$$\frac{d\sigma^B}{d\Omega_\mu dq_+ dq_- d\varphi_\gamma} = \frac{\alpha^3}{2\pi^2 s} A, \tag{2.16}$$

with [7]

$$\begin{aligned} A = & -\frac{m_e^2}{2s'^2} \left( \frac{t^2 + u^2}{(p_- \cdot k)^2} + \frac{t'^2 + u'^2}{(p_+ \cdot k)^2} \right) - \frac{m_\mu^2}{2s^2} \left( \frac{t^2 + u'^2}{(q_- \cdot k)^2} + \frac{t'^2 + u^2}{(q_+ \cdot k)^2} \right) \\ & + \frac{t^2 + t'^2 + u^2 + u'^2}{4ss'} \left[ \frac{s}{(p_+ \cdot k)(p_- \cdot k)} + \frac{s'}{(q_+ \cdot k)(q_- \cdot k)} - \frac{t}{(p_+ \cdot k)(q_+ \cdot k)} \right. \\ & \left. - \frac{t'}{(p_- \cdot k)(q_- \cdot k)} + \frac{u'}{(p_- \cdot k)(q_+ \cdot k)} + \frac{u}{(p_+ \cdot k)(q_- \cdot k)} \right], \end{aligned} \tag{2.17}$$

and

$$\begin{aligned} t &= (p_+ - q_+)^2, & u' &= (p_- - q_+)^2, & s &= (p_+ + p_-)^2, \\ t' &= (p_- - q_-)^2, & u &= (p_+ - q_-)^2, & s' &= (q_+ + q_-)^2. \end{aligned} \tag{2.18}$$

In this expression for  $\sigma^B$  terms of  $O(m_e^2/E^2)$  and  $O(m_\mu^2/E^2)$  have been neglected except where denominators can take the same small values. The terms arising from initial state radiation, final state radiation and the interference of the two can be easily recognized.

### 3. Analytical expressions for certain distributions

In this section analytical results will be given for  $d\sigma/d\Omega_\mu dk$ ,  $d\sigma/dk$ ,  $d\sigma/dq_+^0$  and  $\sigma_{\text{tot}}$ . The first distribution is useful for reproducing the standard radiative corrections. Moreover, it can be used to generate events numerically according to the procedure of sect. 4. Using numerically generated events one can obtain all other distributions. Nevertheless, we give here the analytic expressions for  $d\sigma/dk$  and  $d\sigma/dq_+^0$  in order to demonstrate the importance of hard photons and the influence of initial state radiation versus final state radiation on  $d\sigma/dq_+^0$  which is of relevance for the thrust distribution of jet production. An analytical expression for  $\sigma_{\text{tot}}$  also gives a good idea of the size of the bremsstrahlung correction.

For the  $d\sigma/d\Omega_\mu dk$  distribution we have to integrate (2.15) over  $d\Omega_\gamma$ . As a coordinate system we use the  $\mathbf{q}_+$  momentum as  $z$ -axis and  $\mathbf{q}_+ \wedge \mathbf{p}_+$  as  $y$ -axis. The angles  $\theta_\gamma$  and  $\varphi_\gamma$  are the polar and azimuthal angles of the photon momentum  $\mathbf{k}$ . For the integration it is useful to separate (2.17) into five parts, originating from the electron mass term, muon mass term, the remaining initial state radiation, final state radiation and the electron-muon interference part. The latter gives a contribution to the forward-backward asymmetry. We write accordingly

$$\frac{d\sigma}{d\Omega_\mu d\Omega_\gamma dk} = \frac{\alpha^3}{8\pi^2 s} (X_{m_e} + X_{m_\mu} + X_e + X_\mu + X_{\text{int}}), \quad (3.1)$$

where the functions  $X$  can be written in appropriate forms for the integration:

$$X_{m_e} = -\frac{4m^2 kk'}{(\hat{\mathbf{p}}_+ \cdot \hat{\mathbf{k}})^2} \left( \frac{2c_+^2}{y^4} - \frac{2c_+}{y^3} + \frac{1}{y^2} \right) + (c \rightarrow -c), \quad (3.2)$$

$$X_{m_\mu} = -\frac{2\mu^2 kk' c_s}{y^2} \left( \frac{1}{(\hat{\mathbf{q}}_+ \cdot \hat{\mathbf{k}})^2} + \frac{1}{(\hat{\mathbf{q}}_- \cdot \hat{\mathbf{k}})^2} \right), \quad (3.3)$$

$$X_e = \frac{1}{(\hat{\mathbf{p}}_+ \cdot \hat{\mathbf{k}})} \left( \frac{16k'^2 c_s}{y^4} - \frac{8y_- k'}{y^3} + \frac{4(1+k'^2)}{y^2} \right) + (c \rightarrow -c) - \frac{4k}{y^2}, \quad (3.4)$$

$$\begin{aligned} X_\mu &= \frac{2kk'}{y^2} \frac{1}{(\hat{\mathbf{q}}_+ \cdot \hat{\mathbf{k}})(\hat{\mathbf{q}}_- \cdot \hat{\mathbf{k}})} \{ 2k^2 \sin^2 \theta \sin^2 \theta_\gamma \cos^2 \varphi_\gamma \\ &\quad + (4k^2 c \sin \theta \cos \theta_\gamma \sin \theta_\gamma + 4kxc \sin \theta_\gamma \sin \theta) \cos \varphi_\gamma \\ &\quad + 4x^2 c_s + 8(1-x-k) + 4kx(1+c^2 \cos \theta_\gamma) + 2k^2(1+c^2 \cos^2 \theta_\gamma) \}, \quad (3.5) \end{aligned}$$

$$\begin{aligned} X_{\text{int}} &= \frac{k}{y^2} \left[ \left( \frac{c_-}{\hat{\mathbf{q}}_+ \cdot \hat{\mathbf{k}}} - \frac{c_+}{\hat{\mathbf{q}}_- \cdot \hat{\mathbf{k}}} \right) \left( \frac{4x^3 c_s - 4x^2 y_- c + 4x(1+k'^2)}{(\hat{\mathbf{p}}_+ \cdot \hat{\mathbf{k}})} - 2x(\hat{\mathbf{p}}_- \cdot \hat{\mathbf{k}}) - 4x^2 c \right) + 4xc \right. \\ &\quad \left. - \frac{16k'^2 c_s}{y^2(\hat{\mathbf{p}}_+ \cdot \hat{\mathbf{k}})} + \frac{8y_- k'}{y(\hat{\mathbf{p}}_+ \cdot \hat{\mathbf{k}})} - \frac{4(1+k'^2)}{(\hat{\mathbf{p}}_+ \cdot \hat{\mathbf{k}})} + 2(\hat{\mathbf{p}}_- \cdot \hat{\mathbf{k}}) \right] - (c \rightarrow -c). \quad (3.6) \end{aligned}$$

The notation  $(c \rightarrow -c)$  means that the previous expression should be added with  $c$

replaced by  $-c$  and  $\varphi_\gamma$  by  $\varphi_\gamma + \pi$ . In eqs. (3.1)–(3.6) dimensionless quantities have been used, i.e., for masses and the photon energy

$$m = \frac{m_e}{E}, \quad \mu = \frac{m_\mu}{E}, \quad k = \frac{k^0}{E}, \quad k' = 1 - k = \frac{s'}{s}, \quad (3.7)$$

for 4-momenta

$$\hat{p}_\pm = p_\pm/E, \quad \hat{q}_\pm = q_\pm/E, \quad \hat{k} = k/E. \quad (3.8)$$

For the muon energies we have

$$x = \frac{q_+^0}{E} \approx \frac{2k'}{y}, \quad x' = \frac{q_-^0}{E} = 2 - x - k, \quad (3.9)$$

with

$$y = 2 - k + k \cos \theta_\gamma.$$

The following other notations have been used:

$$c_\pm = 1 \pm c, \quad c_s = 1 + c^2, \quad y_{\pm c} = 2 - k \pm kc. \quad (3.10)$$

It should be noted that in eq. (3.9) the muon mass has been neglected. The exact relation is

$$x = \frac{2k'(2-k) - k \cos \theta_\gamma [4k'^2 + \mu^2(k^2 \cos^2 \theta_\gamma - (2-k)^2)]^{1/2}}{(2-k)^2 - k^2 \cos^2 \theta_\gamma}. \quad (3.11)$$

For  $\cos \theta_\gamma = \mp 1$  this exact relation becomes simple:

$$x(\cos \theta_\gamma = \mp 1) = \frac{1}{2} \left( 2 - k \pm k \left( 1 - \frac{\mu^2}{k'} \right)^{1/2} \right) \approx \begin{cases} 1 - \Delta \\ 1 - k + \Delta \end{cases}, \quad (3.12)$$

with

$$\Delta = \frac{\mu^2 k}{4k'}. \quad (3.13)$$

The maximum  $k$ -value for which the photon can still be isotropically emitted is

$$k_{\max}^{\text{iso}} = \frac{2 - 2\mu}{2 - \mu} \approx 1 - \frac{1}{2}\mu, \quad (3.14)$$

whereas the real maximum photon energy is

$$k_{\max} = 1 - \mu^2. \quad (3.15)$$

For  $\cos \theta_\gamma = \pm 1$ , eq. (3.9) is a good approximation even up to  $k_{\max}^{\text{iso}}$ , as follows from eq. (3.12). However, for general  $\theta_\gamma$  values (3.9) is only a good approximation to (3.11) – within 1% – when

$$k < 1 - 5\mu. \quad (3.16)$$

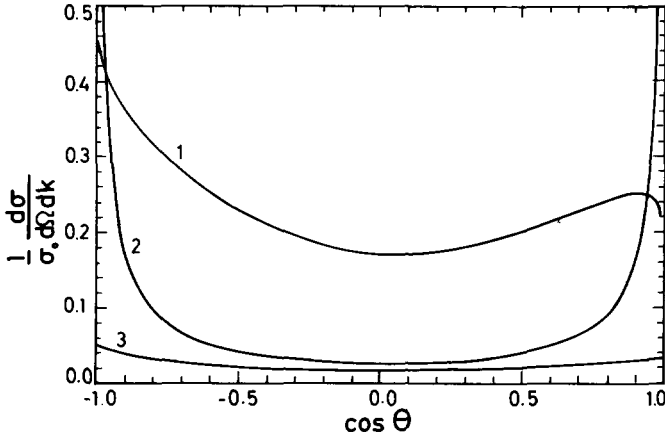


Fig. 1. The distribution  $\sigma_0^{-1} d\sigma/d\Omega_\mu dk$  versus  $\cos \theta$  for three different values of  $k$ : (1)  $k = 0.05$ , (2)  $k = 0.95$  and (3)  $k = 0.5$  for  $E = 15$  GeV.

It should be noted that for  $k > k_{\max}^{\text{iso}}$  there are, in fact, 2 solutions for  $x$ , the one given in (3.11) and one where the sign of  $\cos \theta_\gamma$  is changed. In the range (3.16) we shall perform the integrations. When using (3.9) in the propagators for the muons one should either use the real boundaries (3.12) in the integration, or neglect  $\Delta$  in the boundaries [as (3.9) tells] but use the modified expressions

$$\begin{aligned} \hat{q}_- \cdot \hat{k} &= 2(1 - x + \Delta), \\ \hat{q}_+ \cdot \hat{k} &= 2(x - k' + \Delta), \end{aligned} \tag{3.17}$$

where  $\Delta$  has been added.

3.1. THE DISTRIBUTION  $d\sigma/d\Omega_\mu dk$

$$\frac{d\sigma}{d\Omega_\mu dk} = \frac{\alpha^3}{8\pi^2 s} (Z_{m_e} + Z_{m_\mu} + Z_e + Z_\mu + Z_{\text{int}}), \tag{3.18}$$

where the functions  $Z$  are given in the appendix. The  $\varphi_\gamma$  integral has been performed over the full  $[0, 2\pi]$  interval. The  $\cos \theta_\gamma$  boundaries can still be chosen in such a way that they correspond to a specific acollinearity requirement for the muons. For the case where the full  $\cos \theta_\gamma$  integration is carried out, the angular distribution (3.18) is shown in fig. 1 for a set of  $k$ -values. For very high  $k$ -values this distribution takes the form of the  $e^+e^- \rightarrow \gamma\gamma$  angular distribution, which is understandable for hard photon emission from the initial state. As a comparison the angular distribution for the lowest order process with virtual and soft corrections [eq. (2.1)] is shown in fig. 2.



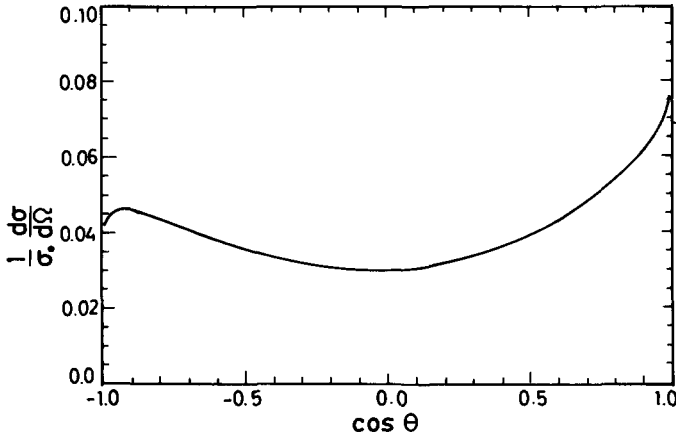


Fig. 2. The distribution  $\sigma_0^{-1} d\sigma/d\Omega_\mu$  according to eq. (2.1) with  $k_1 = 0.01E$  with  $E = 15 \text{ GeV}$ .

### 3.2. THE DISTRIBUTION $d\sigma/dk$

In principle, this distribution can be obtained from (3.18) by integration over  $\cos \theta$ . The interference part gives zero and the muon part is easily obtained from integrating (A.41) and (A.42). The electron part is harder to obtain in this way. It is easier to perform first the  $\varphi_\gamma$  and  $c$  integral, giving rise to eqs. (A.44) and (A.45) and then to perform the  $\cos \theta$ , integral. The resulting distributions are

$$\frac{d\sigma}{dk} = \frac{d\sigma^e}{dk} + \frac{d\sigma^\mu}{dk}, \tag{3.19}$$

where

$$\frac{d\sigma^e}{dk} = \sigma_0 \beta_i \left( \frac{1}{k} + \frac{1}{2k'} - \frac{1}{2} \right), \tag{3.20}$$

$$\frac{d\sigma^\mu}{dk} = \sigma_0 \left( \frac{1}{k} - 1 + \frac{1}{2}k \right) \left( \beta_f + \frac{2\alpha}{\pi} \ln k' \right). \tag{3.21}$$

In fig. 3 the above three quantities are shown.

### 3.3. THE TOTAL CROSS SECTION

We first calculate the contribution in the interval  $[k_1, k_2]$ , where  $k_1$  is a value below which eq. (2.1) is valid and  $k_2 = 1 - 5\mu$ . Therefore,  $k_1$  can be neglected everywhere except in  $\ln k_1$ :

$$\sigma^e = \sigma_0 \beta_i \left[ \ln \left( \frac{k_2}{k_1} \right) - \frac{1}{2} \ln (1 - k_2) - \frac{1}{2} k_2 \right], \tag{3.22}$$

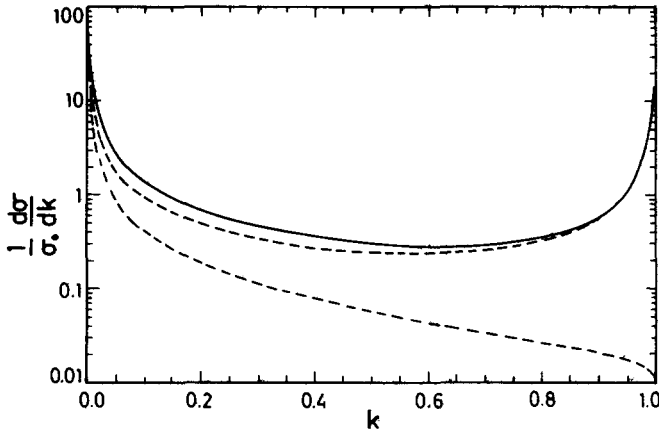


Fig. 3. The photon spectrum  $\sigma_0^{-1} d\sigma/dk$  according to eq. (3.19) (solid curve) and the photon spectrum due to initial state (upper line) and due to final state radiation (lower line) for  $E = 15$  GeV.

$$\sigma^\mu = \sigma_0 \left[ \beta_f \left( \ln \left( \frac{k_2}{k_1} \right) - k_2 + \frac{1}{4} k_2^2 \right) + \frac{\alpha}{\pi} \left( -2 \text{Li}_2(k_2) + \frac{1}{2} (1 - k_2)(3 - k_2) \ln(1 - k_2) + \frac{3}{2} k_2 - \frac{1}{4} k_2^2 \right) \right]. \quad (3.23)$$

When adding the virtual corrections to these expressions (electron loop to  $\sigma^e$ , muon loop to  $\sigma^\mu$ ) we find for the total cross section with a radiated photon energy less than  $k_2$ :

$$\sigma^e(k < k_2) = \sigma_0 \left[ \beta_f \left( \ln k_2 - \frac{1}{2} \ln(1 - k_2) - \frac{1}{2} k_2 \right) + \frac{\alpha}{\pi} \left( \frac{13}{6} \ln \frac{s}{m_e^2} + \frac{1}{3} \pi^2 - \frac{28}{9} \right) \right], \quad (3.24)$$

$$\sigma^\mu(k < k_2) = \sigma_0 \left[ \beta_f \left( \ln k_2 - k_2 + \frac{1}{4} k_2^2 \right) + \frac{\alpha}{\pi} \left( \frac{13}{6} \ln \frac{s}{m_\mu^2} + \frac{1}{3} \pi^2 - \frac{28}{9} - 2 \text{Li}_2(k_2) + \frac{1}{2} (1 - k_2)(3 - k_2) \ln(1 - k_2) + \frac{3}{2} k_2 - \frac{1}{4} k_2^2 \right) \right]. \quad (3.25)$$

The total cross section up to  $k_2$  is given by

$$\sigma(k < k_2) = \sigma_0(1 + \delta_\tau + \delta_{\text{had}}) + \sigma^e(k < k_2) + \sigma^\mu(k < k_2). \quad (3.26)$$

In case one wants to neglect final state radiation, one should take

$$\sigma(k < k_2) = \sigma_0(1 + \delta_\mu + \delta_\tau + \delta_{\text{had}}) + \sigma^e(k < k_2). \quad (3.27)$$

In the region  $1 - 5\mu < k < 1 - \mu^2$  the behaviour of  $d\sigma^\mu/dk$  is smooth and therefore the contribution to the total cross section negligible. The latter can be obtained by taking  $k_2 \rightarrow 1$ . For the electron part this is not the case. In order to evaluate the contribution of  $d\sigma^e/dk$  in this region to the total cross section, we use the reasoning of Bonneau and Martin [8] to get the initial state radiation cross section (cf. appendix)

$$\frac{d\sigma^e}{dk} = \beta_i \sigma_0(s') \left( \frac{1}{k} + \frac{1}{2k'} - \frac{1}{2} \right). \quad (3.28)$$

This equation has neglected some  $m^2$  terms but is still exact as far as  $\mu^2$  terms are concerned. When we now do the same for  $\sigma_0(s')$ , we have instead of (2.8)

$$\sigma_0(s') = \frac{4\pi\alpha^2}{3s} \left( 1 - \frac{\mu^2}{k'} \right)^{1/2} \left( \frac{1}{k'} + \frac{\mu^2}{2k'^2} \right). \quad (3.29)$$

We see that for small  $\mu$  [eq. (2.5)] and  $k$  in the region (3.16) the previous distribution (3.20) is reproduced. Integrating (3.28) from  $k_2$  to  $k_{\max}$  with the help of (3.29), and adding this to (3.22) we find

$$\sigma^e = \sigma_0 \beta_i \left( \ln \frac{1}{k_1} + \frac{1}{2} \ln \frac{s}{m_\mu^2} - \frac{4}{3} \right). \quad (3.30)$$

Insertion of  $k_{\max}$  in eq. (3.22) gives a result which differs in the constant (not  $k_1$  and  $\mu^2$  dependent) terms. It should be noted that our result disagrees with that of ref. [9], where instead of  $-\frac{4}{3}$  the number  $-\frac{19}{12}$  is obtained. The total muon bremsstrahlung for  $k > k_1$  now reads

$$\sigma^\mu = \sigma_0 \left[ \beta_f \left( \ln \frac{1}{k_1} - \frac{3}{4} \right) + \frac{\alpha}{\pi} \left( -\frac{1}{3}\pi^2 + \frac{5}{4} \right) \right]. \quad (3.31)$$

Adding the virtual corrections, one finds for the total cross section for  $\mu^+\mu^-$  and  $\mu^+\mu^-\gamma$  final states the expression

$$\sigma_{\text{tot}} = \sigma_0(1 + \delta_T) = \sigma_0(1 + \delta_e^\Gamma + \delta_\mu^\Gamma + \delta_\tau + \delta_{\text{had}}), \quad (3.32)$$

where

$$\delta_e^\Gamma = \beta_i \left( \frac{1}{2} \ln \frac{4}{\mu^2} - \frac{1}{4} \right) + \frac{2\alpha}{\pi} \left( \frac{1}{6}\pi^2 - \frac{17}{36} \right), \quad (3.33)$$

$$\delta_\mu^\Gamma = \frac{2\alpha}{\pi} \left( \frac{1}{3} \ln \frac{4}{\mu^2} - \frac{13}{72} \right), \quad (3.34)$$

where  $\delta_e^\Gamma$  contains the electron vacuum polarization and  $\delta_\mu^\Gamma$  the muon vacuum polarization. Omitting the latter, one would obtain from vertex correction and bremsstrahlung alone

$$\bar{\delta}_\mu^\Gamma = \frac{3\alpha}{4\pi}, \quad (3.35)$$

TABLE 1

Total correction to the lowest order total cross section in % for the processes  $e^+e^- \rightarrow \mu^+\mu^-$ ,  $e^+e^- \rightarrow \tau^+\tau^-$  denoted by  $\delta_T(\mu)$  and  $\delta_T(\tau)$ , respectively

Contr. (%)	Energy (GeV)	10	25	50	100
	$\delta_e$		3.0	3.3	3.5
$\delta_\mu$		1.4	1.7	1.9	2.1
$\delta_\tau$		0.5	0.8	1.0	1.2
$\delta_{\text{had}}$		4.3	5.6	6.6	7.5
$\overline{\delta_e^T}(\mu)$		44.3	57.6	68.7	80.7
$\overline{\delta_\mu^T}$		0.2	0.2	0.2	0.2
$\overline{\delta_T}(\mu)$		53.7	69.2	81.9	95.4
$\overline{\delta_e^T}(\tau)$		17.8	28.8	38.1	48.3
$\overline{\delta_T}(\tau)$		27.2	40.4	51.3	63.0

The various contributions to the total correction are also listed.

which is a well-known result from the gluon bremsstrahlung to the total QCD cross section (the factor  $\frac{3}{4}$  being cancelled by colour):

$$\sigma_{\text{tot}} = R\sigma_0 \left( 1 + \frac{\alpha_s}{\pi} \right) = R\sigma_0(1 + \delta_{\text{QCD}}). \quad (3.36)$$

At this point it is useful to illustrate numerically the implications of the total cross-section formulae.

In table 1  $\delta_T$  is given for various beam energies both for mu-pair and  $\tau$ -pair production. Moreover, the various contributions to  $\delta_T$  are given, i.e., the leptonic and hadronic vacuum polarizations  $\delta_e$ ,  $\delta_\mu$ ,  $\delta_\tau$ ,  $\delta_{\text{had}}$ , the vertex correction and bremsstrahlung for the initial state  $\overline{\delta_e^T}$  and final state  $\overline{\delta_\mu^T}$ . The latter are (3.33) and (3.34) without  $\delta_e$ ,  $\delta_\mu$ , respectively. The large difference between the total corrections for mu-pair and  $\tau$ -pair production is entirely due to the  $\frac{1}{2}\beta_i \ln(4/\mu^2)$  term in (3.33). It is clear from the table that for the correction to the total cross section the vertex correction and bremsstrahlung for the final state can be neglected.

With these large corrections it is of interest to see which regions of phase space give the large contributions. Table 2 lists  $\delta_T$  for mu-pair production for various maximum photon energies and  $\mu^+$  angular ranges. In the latter case the lowest order cross section to which the correction applies is similarly reduced in angular range. The hard bremsstrahlung region is responsible for the large correction, as was already clear from the difference between mu- and  $\tau$ -pair production.

The formulae for the total mu-pair cross section can also be used to obtain a rough estimate of the total correction to the hadronic cross section. The hadronic cross section can be taken as  $R\sigma_0$ , where  $R(s')$  is roughly a step function with the following  $w' = \sqrt{s'}$  intervals: (0.28, 1), (1, 1.5), (1.5, 4.5), where in the first interval the  $\rho$

TABLE 2

Total correction to the lowest order cross section in % for the process  $e^+e^- \rightarrow \mu^+\mu^-$ , as a function of the photon energy range and the  $\mu^+$  scattering angle range

$k_{\max}$	$E$ (GeV)	10	25	50	100
	$\theta$ range ( $^\circ$ )				
0.95	0-180	26.1	29.7	32.4	35.0
	1-179	26.1±0.3	29.6±0.4	32.4±0.5	35.0±0.6
	10-170	25.4±0.3	29.0±0.4	31.7±0.4	34.2±0.4
	30-150	23.4±0.2	26.7±0.3	29.3±0.3	31.7±0.3
0.8	0-180	18.4	21.2	23.4	25.4
	1-179	18.8±0.3	21.2±0.3	23.3±0.3	25.4±0.3
	10-170	18.7±0.3	21.1±0.3	23.2±0.3	25.3±0.3
	30-150	18.0±0.3	20.5±0.2	22.6±0.2	24.6±0.3
0.5	0-180	10.0	12.0	13.5	14.9
	1-179	10.0±0.2	11.8±0.2	13.4±0.2	14.8±0.2
	10-170	10.2±0.2	11.9±0.2	13.4±0.2	14.8±0.2
	30-180	10.1±0.2	11.9±0.5	13.4±0.2	14.7±0.2

The values for the full angular range are obtained from eq. (3.26), for the restricted range a numerical integration of eq. (3.18) has been performed.

dominates, in the second and third  $R \approx 1, 2$  respectively. Above 4.5 GeV,  $R \approx 4$ . Since we apply the  $\delta_T$  at high energies, the decrease of  $R$  towards lower energies implies a reduction of  $\delta_T$  with respect to the pure mu-pair case. The contribution of the  $\rho$ -meson is given by

$$\sigma^e(\rho\text{-meson}) = \sigma_{\text{had}}\beta_i \frac{9\Gamma_e\pi}{2\alpha^2 MR(s)}. \tag{3.37}$$

For a beam energy of 10 GeV, the correction  $\delta_T$  to  $\sigma_{\text{had}} = R\sigma_0$  is roughly 38%. Of course, an accurate numerical integration of (3.28) with the known hadronic cross section is preferable.

For hadron production it may be of more interest to see which photon angular ranges mainly contribute to the correction. When one excludes in the bremsstrahlung expression (3.28) photons which make an angle of less than  $10^\circ$  with the beam direction, use of eq. (A.53) shows that  $\beta_i$  is reduced by a factor of 4 at 10 GeV. Thus, e.g., when at a beam energy of 10 GeV  $\delta_T$  is 53.7% for mu-pair production, the region  $\frac{2}{3} \leq k \leq k_{\max}$  contributes 40% to this. When in this region photons within  $10^\circ$  of the beam direction are excluded, the total correction becomes 23.7% or, applied to the hadron case mentioned before, the correction of 38% is reduced to 20%. So, in many experimental cases the QED correction will be at least as important as the QCD correction (3.36), which amounts to about 7%.

3.4. THE MOMENTUM SPECTRUM OF THE MUON  $d\sigma/dx$ 

We give here an analytical formula for the  $\mu^+$  momentum distribution caused by initial state radiation. It is obtained, just like  $d\sigma/dk$ , from (A.43)–(A.45), where now an integration over  $k$  has to be performed. For the true momentum spectrum the minimum  $k$ -value is  $1-x$ . If one is interested in the momentum spectrum of the most energetic muon, which is the quantity which may fake a thrust distribution if one does not discard bremsstrahlung events, then the minimum  $k$ -value is  $2(1-x)$ . Since the  $\mu^+$  and  $\mu^-$  momentum distributions are the same a factor 2 also arises in the end result. Thus, the momentum distribution of the most energetic muon becomes

$$\begin{aligned} \frac{d\sigma}{dx} = & \frac{6\alpha\sigma_0}{\pi} \left[ \ln \frac{s}{m_e^2} \left\{ -\frac{2(1-x)^2}{3k_m^3} + \frac{1-x}{k_m^2} - \frac{1+(1-x)^2}{k_m} + \frac{5-6x+3x^2}{6(1-x)} \right. \right. \\ & \left. \left. + x(x-1) \ln \frac{k_m}{2(1-x)} - \frac{1}{2}(x^2+(1-x)^2) \ln \frac{1-k_m}{2x-1} \right\} \right. \\ & \left. + \frac{8(1-x)^2}{3k_m^3} - \frac{4(1-x)}{k_m^2} + \frac{x^2-2x+3}{k_m} - \frac{1}{2}(1-x) - \frac{1}{3(1-x)} \right. \\ & \left. + \frac{1}{2} \ln \frac{1-k_m}{2x-1} - x(x-1) \ln \left[ \frac{k_m}{1-k_m} \frac{2x-1}{2-2x} \right] \right], \quad (3.38) \end{aligned}$$

where  $k_m$  is the maximum photon energy one is interested in. Expression (3.34) should be compared to the thrust distribution, calculated in QCD from gluon bremsstrahlung [10]

$$\frac{1}{\sigma_0} \frac{d\sigma}{dT} = \frac{2\alpha_s}{3\pi} \left[ \frac{2(3T^2-3T+2)}{T(1-T)} \ln \frac{2T-1}{1-T} - \frac{3(3T-2)(2-T)}{1-T} \right]. \quad (3.39)$$

In fig. 4  $d\sigma/dT$  and  $d\sigma/dx$  are presented for various beam energies. The maximum photon energies are chosen in such a way that  $s'$  is still large enough to produce jets ( $\sqrt{s'} > 7$  GeV). In this region  $R(s')$  can be taken constant such that eq. (3.38) can be applied. Again it is seen that QCD and QED effects can be comparable in size.

## 4. A procedure to generate events

When one wants to generate  $x$ -values in an interval  $(a, b)$  according to a prescribed distribution  $f(x)$ , there are various ways to follow. Each method should produce a number  $N(x)$  of points per interval  $\Delta x$  which approaches  $f(x)\Delta x$  for a large total number of generated events.

One method would be to divide the interval  $(a, b)$  into a large number of sub-intervals  $\Delta x_i$ , each of such a size that  $\int_i f(x) dx$  over the interval is of about the same magnitude for every interval. One could then at random generate the number  $i$  and choose a point in  $\Delta x_i$ .

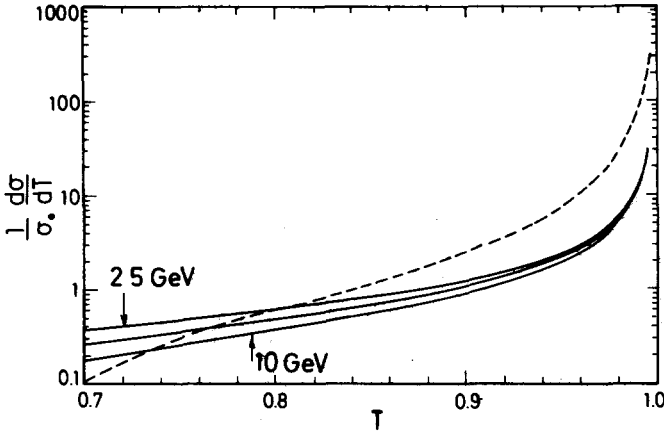


Fig. 4. The thrust distribution  $\sigma_0^{-1} d\sigma/dT$  faked by initial state radiation for three beam energies  $E = 10, 15, 25$  GeV and the QCD thrust distribution  $\sigma_0^{-1} d\sigma/dT$  (dashed line). For the first distribution photon energies are allowed up to that value which gives a  $q\bar{q}$  pair of an invariant mass of 7 GeV.

Another way would be to generate at random points  $(x, y)$ , where  $x \in (a, b)$  and  $y \in (f_1, f_2)$ , where  $f_1$  and  $f_2$  are the minimum and maximum values of  $f$  in the interval  $(a, b)$ . When for a generated point  $(x, y)$   $y < f(x)$ , the value  $x$  is accepted, otherwise not.

A third method is to calculate analytically

$$F(z) = \int_a^z f(x) dx, \tag{4.1}$$

to generate a random number  $\eta \in [0, F(b)]$  and to solve numerically the equation

$$\eta = F(x). \tag{4.2}$$

In the multidimensional case, similar methods can be used. When a differential cross section has narrow and high peaks in various variables, the third approach will have some advantages. The explicit integration amounts effectively to the introduction of new variables so that the distribution becomes flat. Without the explicit integration one could, of course, directly introduce variables which would transform away some peaks, and then use any of the other two methods. However, there are more peaks than variables which can be chosen independently so that some peaks remain in the newly chosen variables.

So, ideally one should perform the five integrations of eq. (2.15) step by step and then generate each kinematical variable by using eqs. (4.1) and (4.2) in five steps. When one wants to do this for eq. (2.15) to the very end, one runs into two problems. The first is that, in a small region above zero photon energy, eq. (2.15) is not applicable and only the cross section integrated over the photon energies is known [eq. (2.1) or (2.6)]. The second problem is that it is not easy to integrate eq. (2.6)

analytically over  $c = \cos \theta$ , so that the procedure with (4.2) cannot be done using analytical equations. Now it is most important to use analytical formulae for those integrals which have the strongest peaks. Those are the  $\varphi_\gamma$  and  $\cos \theta_\gamma$  integrals. Therefore we adopt the following procedure.

In the phase space which is only restricted for  $\theta(c)$ -values by (2.5) and  $k$ -values by (3.16) we use eq. (3.18) from a certain  $k$ -value on and eq. (2.6) for very low  $k$ -values (soft region). A two-dimensional  $k, c$  histogram is created numerically for which integrals like (4.1) are known.

First a  $k$ -value is created; if it is in the soft region, the  $k$ -value is negligible and can be set to zero for experimental purposes. A  $c$ -value is generated from (2.6). Outside the soft region it is eq. (3.18) which gives the  $c$ -value numerically. With the generated  $k, c$ -values it is then possible to use the primitive functions  $Z$  to generate  $\cos \theta_\gamma$  and the functions  $Y$  to generate  $\varphi_\gamma$ .

One improvement to this scheme must be made. When the  $k_1$  value at which the soft region ends is changed, the result is not the same since in the soft region the cross section is changed by exponentiation, whereas in the other part it is not. This problem would not have occurred if eq. (2.1) were used in the soft region. For small  $k$ -values the created events would then, however, be too few. The solution is that (3.18) should be modified in such a way that upon  $k$  integration it obtains a similar factor as eq. (2.6). Writing (3.18) formally as

$$\frac{d\sigma}{d\Omega_\mu dk} = \frac{d\sigma_0}{d\Omega_\mu} \left( \frac{\beta}{k} + \frac{d}{dk} h(k) \right), \quad (4.3)$$

the cross section up to  $k_1$  with exponentiation is assumed to be

$$\frac{d\sigma}{d\Omega_\mu} (k < k_1) = \frac{d\sigma_0}{d\Omega_\mu} (1 + \delta_{AR} + h(k_1)) k_1^\beta. \quad (4.4)$$

Differentiating, we now find for (4.3) the exponentiated version

$$\frac{d\sigma^{ex}}{d\Omega_\mu dk_1} = \frac{d\sigma_0}{d\Omega_\mu} (\delta_{AR} + h(k_1)) \beta k_1^{\beta-1} + \frac{d\sigma}{d\Omega_\mu dk_1} k_1^\beta \quad (4.5)$$

$$= \left( \frac{d\sigma}{d\Omega_\mu dk_1} + \frac{\beta \delta_{AR}}{k_1} \frac{d\sigma_0}{d\Omega_\mu} \right) k_1^\beta. \quad (4.6)$$

For generating events we use (4.6). The term with  $h(k_2)$  is of higher order than the last term and is small in the region where exponentiation is most important. It can therefore be neglected. An evaluation would be involved. It is (4.6) which is used to generate  $k$  and  $c$ . The photon variables are then generated from  $d\sigma/d\Omega_\mu dk$  alone, as described before. The main purpose of this procedure is to redistribute the events for small  $k$ -values, since we know that higher order corrections become necessary there. If one is only interested in hard bremsstrahlung the use of (4.6) is not necessary but using it does not affect the results. As an illustration, the effect of exponentiation



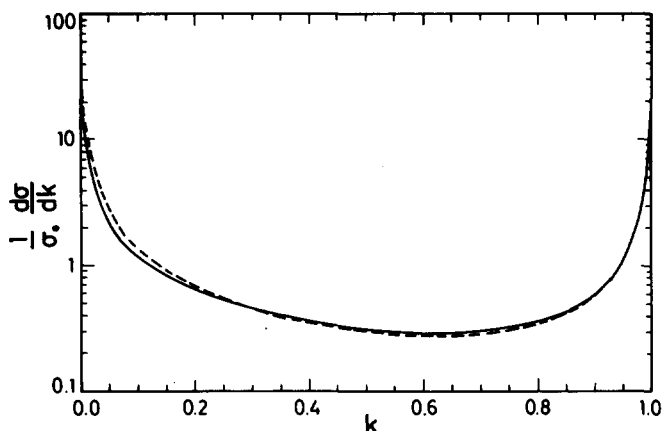


Fig. 5. The photon spectrum with (solid curve) and without (dashed curve) exponentiation for  $E = 15$  GeV.

like in eq. (4.5) is shown for the photon spectrum in fig. 5. In fig. 6 the exponentiated form of  $\sigma(k < k_1)$  is compared to the form without exponentiation.

The distribution (4.6) can also be used for a fixed scattering angle. One then generates the  $k$ -values from a one-dimensional histogram. If one had chosen a different order of integration, this would not have been possible.

If one is exclusively interested in either initial or final state radiation, another order of integration is possible leading, e.g., to eqs. (A.43)–(A.47), for which all primitive functions are known. Then the corresponding transition from (4.5) to (4.6) has not to be made and no starting histogram has to be created. When using the earlier mentioned step-function approximation to  $R(s)$ , it is easy to generate the momenta of a real and a massive virtual photon, which is useful to calculate the radiative

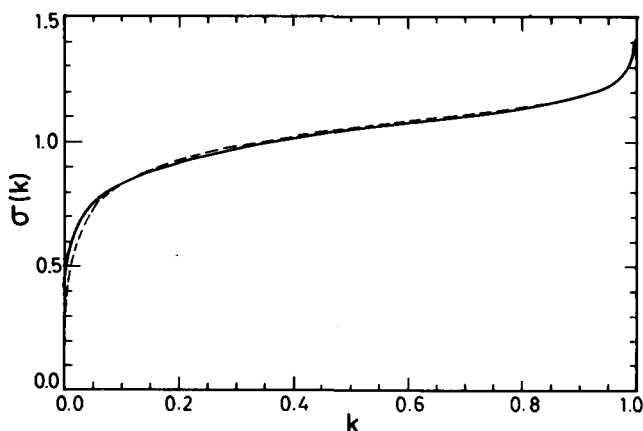


Fig. 6. The integrated photon spectrum  $\sigma(k) = \sigma^o(k) + \sigma^\mu(k)$  with (solid curve) and without (dashed curve) exponentiation, in units of  $\sigma_0$ .

correction to  $\mathcal{R}$ . If one is interested in hadron jets, information on how the virtual photon decays into a  $q\bar{q}$  pair is also required. The chain of integrals leading to (A.43) should then be used in order to generate the 4-momenta of the quark and antiquark. The hadrons coming from the  $q\bar{q}$  pair can then be obtained by using one of the current Monte Carlo programs [11].

## 5. Numerical examples of radiative corrections and distributions

### 5.1. RADIATIVE CORRECTION TO $d\sigma/d\Omega_\mu$

As mentioned in sect. 1, we can use the expressions for  $d\sigma/d\Omega_\mu dk$  to perform numerically an integration over that part of phase space where the muon energies are larger than a prescribed value  $E_{\text{th}}$ :

$$q_+^0, q_-^0 \geq E_{\text{th}}, \quad (5.1)$$

and where the angle between the muons lies in the region

$$\pi - \zeta \leq \angle(\mathbf{q}_+, \mathbf{q}_-) \leq \pi. \quad (5.2)$$

The lowest order differential cross section  $d\sigma_0/d\Omega_\mu$  then obtains a total correction  $\delta_T$ , which contains virtual corrections, hadronic vacuum polarization and bremsstrahlung. The results are in agreement with those of refs. [2, 3, 12]. In fig. 7 the total QED correction  $\delta_T$  is given to which  $\delta_W$  (2.14) should be added to obtain the total electroweak asymmetry (fig. 8). The latter is shown for two energies, the change coming mainly from the weak interference part. This is the only calculation in this paper where  $\delta_W$  is included, everywhere else pure QED with  $\delta_{\text{had}}$  is considered.

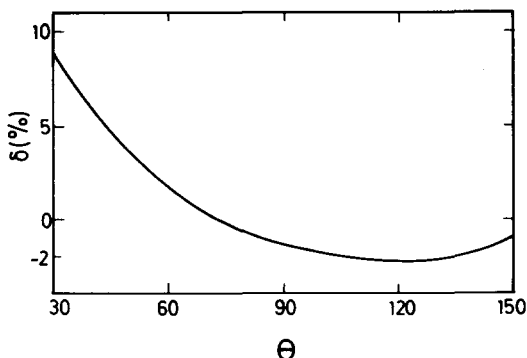


Fig. 7. The total QED radiative correction  $\delta_T$  in % for  $E_{\text{th}} = 0.5E$  and  $\zeta = 10^\circ$  for various scattering angles  $\theta$  and  $E = 15 \text{ GeV}$ .

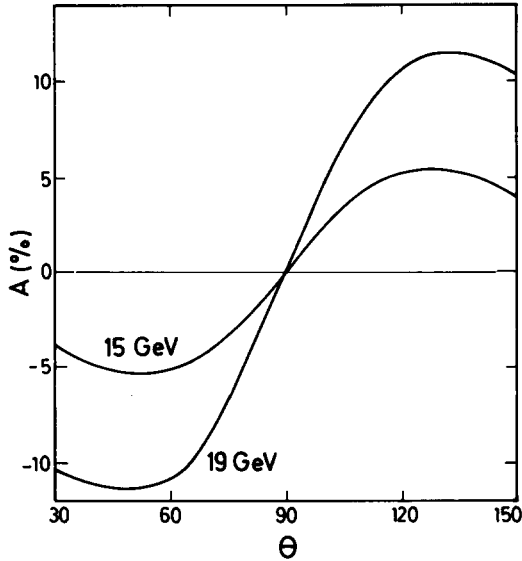


Fig. 8. The forward-backward asymmetry, now including the electroweak interference  $\delta_w$  for  $E = 15$  and  $19$  GeV. The same  $E_{th}$  and  $\zeta$  are used as in fig. 7 and  $\sin^2 \theta_w = 0.22$ .

5.2. THE PHOTON ENERGY DISTRIBUTIONS

Although we have given in sect. 4 an exact distribution, eq. (3.19), which is plotted in fig. 3, the event generator should reproduce the same distribution. Generating 10 000 events in a phase space determined by

$$0.5^\circ \leq \theta \leq 175.5^\circ, \quad 0 \leq k \leq 0.96, \quad (5.3)$$

the photon spectrum is that given in fig. 9. It should be noted that in contrast to eq. (3.19) the region  $(0, k_1)$  with very small  $k_1$  is included in the sample, as was discussed

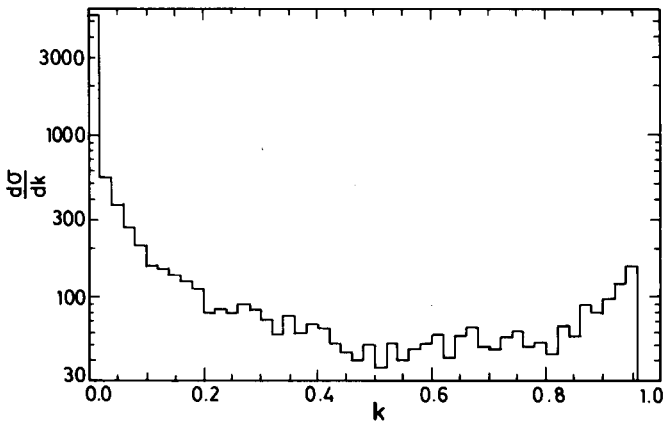


Fig. 9. The photon spectrum, including soft photons, as generated numerically for  $E = 15$  GeV.

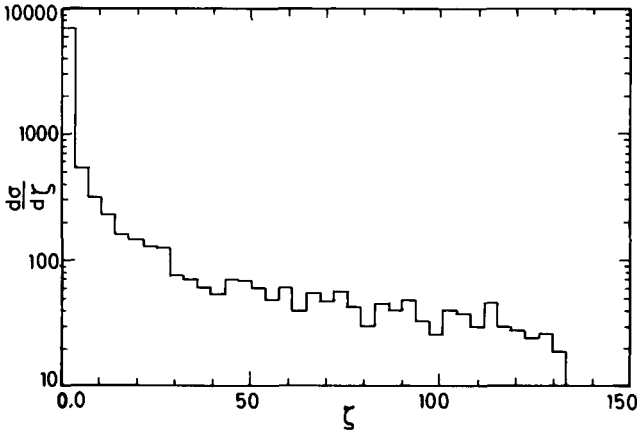


Fig. 10. The numerically generated acollinearity distribution for  $E = 15$  GeV.  $\zeta$  in degrees.

in sect. 4. The agreement between the exact distribution and the generated histogram is good. A similar check was made on fig. 4.

### 5.3. THE ACOLLINEARITY DISTRIBUTION

Using the same event sample as above one can obtain  $d\sigma/d\zeta$ , where  $\zeta$  is the acollinearity angle (5.2). The resulting histogram is depicted in fig. 10.

### 5.4. THE ACOPLANARITY DISTRIBUTION

Defining an acoplanarity angle  $\psi$  between the two planes formed by the beam and the  $\mu^+$ ,  $\mu^-$  respectively, a distribution like the one in fig. 11 is obtained. The angle  $\pi - \psi$  is the angle between  $\mathbf{p}_+ \wedge \mathbf{q}_+$  and  $\mathbf{p}_- \wedge \mathbf{q}_-$ .

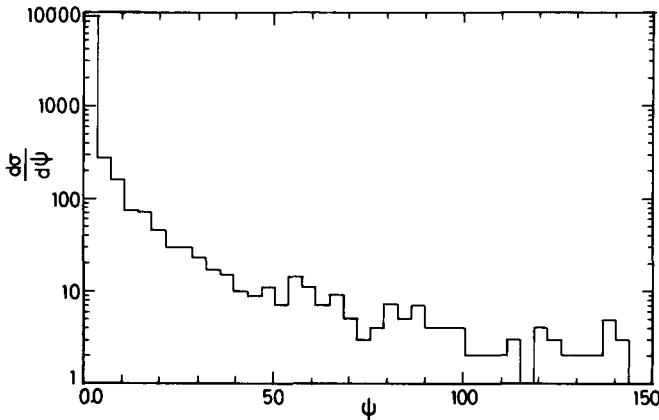


Fig. 11. The acoplanarity distribution as generated numerically for  $E = 15$  GeV.  $\psi$  in degrees.

We would like to thank Drs. Lynch and Newman for stimulating us to look for more general methods of calculating radiative corrections. One of us (R.K.) would like to thank the DESY Theory Group for their kind hospitality. This investigation is part of the research program of the ‘‘Stichting voor Fundamenteel Onderzoek der Materie (F.O.M.)’’.

### Appendix

In this appendix formulae are given relevant for the integration order  $\varphi_\gamma, \cos \theta_\gamma$  and the order  $\varphi_\gamma, c$ . Furthermore, a separate treatment of the initial state radiation only is made.

#### INTEGRATION OVER $\varphi_\gamma$

The functions  $X$  in eq. (3.1) are integrated over  $\varphi_\gamma$ . Denoting the integrals by

$$Y = \int X \, d\varphi_\gamma, \tag{A.1}$$

we find

$$Y_{m_e} = -\frac{4m^2k'}{k} \left[ \left( \frac{2c_+^2}{y^4} - \frac{2c_+}{y^3} + \frac{1}{y^2} \right) I_2^- + \left( \frac{2c_-^2}{y^4} - \frac{2c_-}{y^3} + \frac{1}{y^2} \right) I_2^+ \right], \tag{A.2}$$

$$Y_e = \frac{1}{y^2k} \left[ \left( \frac{16k'^2c_s}{y^2} - \frac{8y_{-c}k'}{y} + 4(1+k'^2) \right) I_1^- + \left( \frac{16k'^2c_s}{y^2} - \frac{8y_{+c}k'}{y} + 4(1+k'^2) \right) I_1^+ - 4k^2I_3 \right], \tag{A.3}$$

where

$$I_1^\mp = \frac{2}{R_\mp^{1/2}} \arctan \left[ \frac{R_\mp^{1/2}}{a_\mp + b_\mp} \tan \left( \frac{1}{2}\varphi_\gamma \right) \right], \tag{A.4}$$

$$I_2^\mp = \frac{1}{R_\mp} \left( -\frac{b_\mp \sin \varphi_\gamma}{a_\mp + b_\mp \cos \varphi_\gamma} + a_\mp I_1^\mp \right), \tag{A.5}$$

$$I_3 = \varphi_\gamma, \tag{A.6}$$

$$a_\mp = \left( \frac{p_+^0}{|p_+|} \right)^\mp c \cos \theta_\gamma \equiv e^\mp c \cos \theta_\gamma, \tag{A.7}$$

$$b_\mp = \mp \sin \theta \sin \theta_\gamma, \tag{A.8}$$

$$R_\mp = a_\mp^2 - b_\mp^2 = (ec \mp \cos \theta_\gamma)^2 + m^2 \sin^2 \theta. \tag{A.9}$$

Furthermore, the muon part gives

$$Y_{m_\mu} = X_{m_\mu} I_3, \quad (\text{A.10})$$

$$Y_\mu = \frac{2kk'}{y^2(\hat{q}_+ \cdot \hat{k})(\hat{q}_- \cdot \hat{k})} [(4x^2 c_s + 8(1-x-k) + k^2 \sin^2 \theta \sin^2 \theta_\gamma) \\ + 2k^2(1+c^2 \cos^2 \theta_\gamma) + 4kx(1+c^2 \cos \theta_\gamma)] I_3 \\ + (x+k \cos \theta_\gamma)(4kc \sin \theta \sin \theta_\gamma) I_4 + (\frac{1}{2}k^2 \sin^2 \theta \sin^2 \theta_\gamma) I_5, \quad (\text{A.11})$$

with

$$I_4 = \sin \varphi_\gamma, \quad (\text{A.12})$$

$$I_5 = \sin 2\varphi_\gamma. \quad (\text{A.13})$$

The interference term reads

$$Y_{\text{int}} = \frac{1}{y^2} \left[ \left( \frac{c_-}{\hat{q}_+ \cdot \hat{k}} - \frac{c_+}{\hat{q}_- \cdot \hat{k}} \right) [(4x^3 c_s - 4x^2 y_{-c} + 4x(1+k'^2)) I_1^- \right. \\ \left. - 2k^2 x((1+c \cos \theta_\gamma) I_3 + \sin \theta \sin \theta_\gamma I_4) - 4x^2 ck I_3] \right. \\ \left. - \left[ \frac{16k'^2 c_s}{y^2} - \frac{8y_{-c} k'}{y} + 4(1+k'^2) \right] I_1^- + 4xkc I_3 \right. \\ \left. + 2k^2 [(1+c \cos \theta_\gamma) I_3 + (\sin \theta \sin \theta_\gamma) I_4] \right] - (c \rightarrow -c). \quad (\text{A.14})$$

The definite integrals over the interval  $[0, 2\pi]$  are obtained from the above expressions by taking

$$I_1^\mp = \frac{2\pi}{R_\mp^{1/2}}, \quad I_2^\mp = \frac{2\pi a_\mp}{R_\mp^{3/2}}, \quad I_3 = 2\pi, \quad I_4 = I_5 = 0. \quad (\text{A.15})$$

#### INTEGRATION OVER $\cos \theta_\gamma$

The definite integrals  $Y$  with eqs. (A.15) inserted are integrated over  $\cos \theta_\gamma$ . The resulting integrals are denoted by  $Z$ :

$$Z = \int Y \, d \cos \theta_\gamma. \quad (\text{A.16})$$

In particular

$$Z_{m_e} = -\frac{8\pi k'}{k} \left( \frac{2c_+^2}{y_+ c} - \frac{2c_+}{y_+ c} + \frac{1}{y_+^2 c} \right) \frac{w}{R_-^{1/2}} + (c \rightarrow -c), \quad (\text{A.17})$$

$$Z_e = \frac{8\pi}{k} [4k'^2 c_s f_4 - 2y_{-c} k' f_3 + (1+k'^2) f_2 + (c \rightarrow -c)] + \frac{8\pi}{y}, \quad (\text{A.18})$$

$$Z_{m_\mu} = \frac{1}{2}\pi c_s \mu^2 \left[ \frac{1}{1-x+\Delta} - \frac{1}{x-k'+\Delta} \right], \quad (\text{A.19})$$

$$Z_\mu = -\pi \left[ c_s \frac{1+k'^2}{k} \ln \left( \frac{x-k'+\Delta}{1-x+\Delta} \right) - 2xc_s + \frac{2k'}{x} (3c^2-1) \right], \quad (\text{A.20})$$

where

$$f_n = \frac{1}{(n-1)a_0^2} (-g_{n-1} + (2n-3)y_0 f_{n-1} - (n-2)f_{n-2}), \quad (n > 1), \quad (\text{A.21})$$

$$g_n = \frac{kR_-^{1/2}}{y^n}, \quad (\text{A.22})$$

$$f_1 = \frac{1}{a_0} \ln \left[ \frac{2y(w + R_-^{1/2})}{(y + a_0 + kR_-^{1/2})^2} \right], \quad (\text{A.23})$$

$$w = \cos \theta_\gamma - ec,$$

$$y_0 = 2 - k + kec, \quad (\text{A.24})$$

$$a_0 = [y_0^2 + k^2 m^2 \sin^2 \theta]^{1/2}.$$

The interference term gives

$$\begin{aligned} Z_{\text{int}} = 4\pi & \left[ 2c_s(c-Q_3 - c_+R_3) - 2(c-Q_2 - c_+R_2)y_{-c} \right. \\ & + 2(1+k'^2)(c-Q_1 - c_+R_1) + \frac{1}{2}kU - \frac{2k'c}{y^2} \\ & - \frac{1}{2}k(c-S_1 - c_+T_1) - kc(c-S_2 - c_+T_2) \\ & \left. - 8k'^2 c_s f_4 + 4y_{-c} k' f_3 - 2(1+k'^2)f_2 \right] - (c \rightarrow -c), \quad (\text{A.25}) \end{aligned}$$

where

$$Q_n = \frac{(2k')^{n-1}}{2(1+\Delta')} f_{n+1} + \frac{k'}{1+\Delta'} Q_{n-1}, \quad (n > 1), \quad (\text{A.26})$$

$$Q_1 = \frac{1}{4(1+\Delta')^2} (2(1+\Delta')f_2 + f_1 - V), \quad (\text{A.27})$$

$$\Delta' = \Delta/k',$$

$$R_n = -\frac{1}{2}(2k')^{n-1} f_{n+1} + (1+\Delta)R_{n-1}, \quad (n > 1), \quad (\text{A.28})$$

$$R_1 = -\frac{1}{2}f_2 - \frac{1+\Delta}{4k'} (f_1 - W), \quad (\text{A.29})$$

$$V = \frac{1}{a_1} \ln \left[ \frac{2y_1(w + R_-^{1/2})}{(y_1 + a_1 + kR_-^{1/2})^2} \right], \quad (\text{A.30})$$

and  $W$  is obtained from  $V$  by replacing  $a_1, y_1$  by  $a_2, y_2$ , where

$$a_1 = [\tilde{y}_1^2 + m^2 k^2 \sin^2 \theta]^{1/2}, \tag{A.31}$$

$$a_2 = [\tilde{y}_2^2 + m^2 k^2 \sin^2 \theta]^{1/2}, \tag{A.32}$$

$$y_1 = y - 2(1 + \Delta'), \quad \tilde{y}_1 = y_0 - 2(1 + \Delta'), \tag{A.33}$$

$$y_2 = y - \frac{2k'}{1 + \Delta}, \quad \tilde{y}_2 = y_0 - \frac{2k'}{1 + \Delta}, \tag{A.34}$$

$$S_1 = -\frac{1}{2} \left[ c_+ \ln(x - k' + \Delta) + \frac{x}{kk'} (kc_+ - 2c) \right], \tag{A.35}$$

$$S_2 = -\frac{1}{2k} \left[ k' \ln(x - k' + \Delta) + x + \frac{x^2}{2k'} \right], \tag{A.36}$$

$$T_1 = \frac{1}{2k'} \left[ c_- \ln(1 - x + \Delta) + \frac{x}{k} (kc_+ - 2c) \right], \tag{A.37}$$

$$T_2 = \frac{1}{2kk'} [\ln(1 - x + \Delta) + x + \frac{1}{2}x^2], \tag{A.38}$$

$$U = -\frac{1}{kk'} [\frac{1}{2}x^2(kc_+ - 2c) + 2cxk']. \tag{A.39}$$

For the definite integrals some simplifications occur. For  $Z_{m_e}$  the  $\cos \theta_\gamma$  dependent factor becomes 2, in  $Z_e$  we have

$$f_1(1) - f_1(-1) = -\frac{1}{a_0} \ln \left( \frac{k'm^2}{y_0^2} \right). \tag{A.40}$$

The muon parts become

$$Z_{m_\mu}(1) - Z_{m_\mu}(-1) = -4\pi c_s \frac{k'}{k} \tag{A.41}$$

$$Z_\mu(1) - Z_\mu(-1) = 2\pi c_s \left( \frac{1+k'^2}{k} \right) \ln \left( \frac{4k'}{\mu^2} \right) - 8\pi c^2 k. \tag{A.42}$$

Next, we give a result which is obtained by integration of  $Y$  over the full  $c$ -range and the azimuthal angle of the  $\mu^+$  (just a factor of  $2\pi$ ):

$$\begin{aligned} \frac{d\sigma}{dk d \cos \theta_\gamma} &= \frac{2kk'}{y^2} \frac{d\sigma}{dk dx} = \frac{2kk'}{y^2} \frac{d\sigma}{dx dx'} \\ &= \frac{\alpha^3}{8\pi^2 s} \int Y d\Omega_\mu \equiv \frac{\alpha^3}{8\pi^2 s} \frac{2kk'}{y^2} H, \end{aligned} \tag{A.43}$$

$$H_{m_e} = \frac{32\pi^2}{k^4} [2k' - x^2 - x'^2], \tag{A.44}$$



$$H_e = \frac{16\pi^2}{k^2 k'} \left[ \ln \frac{s}{m_e^2} \left( x^2 + x'^2 - \frac{4k'}{k^2} (xx' - k') \right) + \frac{1}{k^2} \left( (2k^2 + 12k')(xx' - k') - 2k^2 k' \right) - k^2 \right], \tag{A.45}$$

$$H_{m_\mu} = -\frac{32}{3}\pi^2 \mu^2 \left( \frac{1}{(\hat{q}_+ \cdot \hat{k})^2} + \frac{1}{(\hat{q}_- \cdot \hat{k})^2} \right), \tag{A.46}$$

$$H_\mu = \frac{16}{3}\pi^2 \frac{4}{(\hat{q}_+ \cdot \hat{k})(\hat{q}_- \cdot \hat{k})} (x^2 + x'^2). \tag{A.47}$$

When the photon direction is not near to the  $\mu^\pm$  direction,  $H_{m_\mu}$  can be neglected. These formulae are in agreement with those of ref. [9].

To conclude, we give some formulae relevant for the initial state radiation. Using now  $\mathbf{p}_+$  as  $z$ -axis, calling the polar and azimuthal angle of the photon  $\eta$  and  $\psi$  and denoting  $k^0/E$  by  $k$  we have

$$\frac{d\sigma^e}{d\Omega_\gamma dk} = \frac{\alpha k}{4\pi^2} \sigma_0(s') \left[ \frac{2(1+k'^2)}{(\hat{p}_+ \cdot \hat{k})(\hat{p}_- \cdot \hat{k})} - \frac{m^2 k'}{(\hat{p}_+ \cdot \hat{k})^2} - \frac{m^2 k'}{(\hat{p}_- \cdot \hat{k})^2} - 1 \right]. \tag{A.48}$$

Integrating over the full  $\psi$  range and then integrating over  $\cos \eta$  gives

$$\frac{d\sigma}{dk} = \frac{\alpha}{2\pi k} \sigma_0(s') [-m^2 k' J_1 - k^2 J_2 + (1+k'^2) J_3], \tag{A.49}$$

with

$$\begin{aligned} J_1 &= \frac{1}{e - \cos \eta} - \frac{1}{e + \cos \eta}, \\ J_2 &= \cos \eta \\ J_3 &= \ln \left( \frac{e + \cos \eta}{e - \cos \eta} \right). \end{aligned} \tag{A.50}$$

For the interval  $(-1, +1)$  the integrals  $J_i$  give

$$J_1 = \frac{4}{m^2}, \quad J_2 = 2, \quad J_3 = 2 \ln \frac{s}{m_e^2}, \tag{A.51}$$

and therefore

$$\frac{d\sigma^e}{dk} = \frac{\alpha}{\pi} \sigma_0(s') \left( \ln \frac{s}{m_e^2} - 1 \right) \frac{1+k'^2}{k}, \tag{A.52}$$

which is the same as (3.28). For a restricted angular range, e.g.,  $(-z, z)$  we obtain instead of (A.52)

$$\frac{d\sigma^e}{dk} = \frac{\alpha}{\pi} \sigma_0(s') \left( \frac{1+k'^2}{k} \ln \left( \frac{e+z}{e-z} \right) - kz \right). \tag{A.53}$$

## References

- [1] S. Glashow, Nucl. Phys. 22 (1961) 579;  
S. Weinberg, Phys. Rev. Lett. 19 (1967) 1264;  
A. Salam, in Elementary particle theory, ed. N. Svartholm (Almqvist and Forlag, Stockholm, 1968)
- [2] F.A. Berends, K.J.F. Gaemers and R. Gastmans, Nucl. Phys. B57 (1973) 381
- [3] F.A. Berends, K.J.F. Gaemers and R. Gastmans, Nucl. Phys. B63 (1973) 381
- [4] F.A. Berends and R. Gastmans, in Electromagnetic interactions of hadrons, vol. 2, p. 471, ed. A. Donnachie and G. Shaw (Plenum, 1978)
- [5] F.A. Berends and G.J. Komen, Phys. Lett. 63B (1976) 432
- [6] G. Passarino and M. Veltman, Nucl. Phys. B160 (1979) 151
- [7] F.A. Berends, R. Gastmans and T.T. Wu, University of Leuven preprint KUL-TF-79/022, submitted to 1979 Int. Symp. on Lepton and photon interactions at high energies, 1979, Fermilab
- [8] G. Bonneau and F. Martin, Nucl. Phys. B27 (1971) 381
- [9] E.A. Kuraev and G.V. Meledin, Nucl. Phys. B122 (1977) 485
- [10] A. de Rújula, J. Ellis, E.G. Floratos and M.K. Gaillard, Nucl. Phys. B138 (1978) 387
- [11] A. Ali, E. Pietarinen, G. Kramer and J. Willrodt, DESY report 79/86
- [12] G.J. Komen, Phys. Lett 68B (1977) 275